European Journal of Pharmaceutical Sciences 87 (2016) 58–68

Contents lists available at ScienceDirect

European Journal of Pharmaceutical Sciences

journal homepage: www.elsevier.com/locate/ejps

Pharmacokinetics, tissue distribution and excretion of 40 kDa PEG and PEGylated rFVIII (N8-GP) in rats

Inga Bjørnsdottir *, Ola Sternebring, Wendela A. Kappers, Helle Selvig, Hanne T. Kornø, Jesper B. Kristensen, Morten A. Bagger

Development DMPK and Isotope Chemistry, Novo Nordisk A/S, Novo Nordisk Park, Måløv, Denmark

ARTICLE INFO

Article history:
Received 8 July 2015
Received in revised form 21 October 2015
Accepted 25 October 2015
Available online 27 October 2015

Keywords:
Distribution
Excretion
N8-GP
PEGylated rFVIII
Pharmacokinetics

ABSTRACT

The biologic fate of the [^{3}H]PEG-moiety incorporated into N8-GP was evaluated based on single i.v. bolus doses to rats. Furthermore, the 40 kDa [^{3}H]PEG-moiety was given separately to rats by single i.v. bolus doses, to investigate if the pharmacokinetics were dose-dependent. For both compounds, plasma pharmacokinetics, distribution and excretion pathways were investigated, based on total radioactivity measurements ([^{3}H]N8-GP: 0.17–4.1 mg/kg;~1300–30,000 U/kg, PEG load of ~0.03–0.7 mg/kg); ([^{3}H]PEG: 0.6, 1, 12, 100 and 200 mg/kg). The plasma concentration of the intact N8-GP conjugate was also measured by ELISA. After single i.v. administration to rats, both [^{3}H]N8-GP and [^{3}H]PEG were shown to be widely distributed, mainly in highly vascularized tissues, with the lowest levels of radioactivity found in the CNS. Though a slow elimination of radioactivity was observed over the 12-week study period, approximately half of the radioactive dose of either compound was removed from the body 1 week post-dose. The radioactivity was eliminated mainly via the kidney into urine but also via the liver into feces, with a larger fraction found in the feces for [^{3}H]N8-GP. Elimination of the 40 kDa PEG-moiety was shown to be dose-dependent with faster elimination at lower dose levels. The clinical dose of N8-GP provides a substantially lower PEG exposure (50–75 U/kg; PEG load of <0.002 mg/kg) when compared to the PEG doses investigated in this paper (0.03–200 mg/kg). This may imply an even faster clearance of the PEG-moiety after N8-GP administration of clinically relevant doses.

1. Introduction

Hemophilia A, the most common type of hemophilia, is an inherited bleeding disorder caused by a deficiency in, or dysfunction of, coagulation factor VIII (FVIII). Hemophilia A is often treated by intravenous (i.v.) injections of either FVIII purified from human plasma or FVIII produced using recombinant DNA technology. Based on decades of clinical experience in severe hemophilia (Nilsson et al., 1992), prophylactic treatment is currently recommended as the first choice of treatment for severe hemophilia A by the World Federation of Hemophilia (Srivastava et al., 2013) and the Medical and Scientific Advisory Council of the National Hemophilia Foundation (MASAC Recommendation Concerning Prophylaxis. Document #179, 2007). The scope is to prevent frequent and/or prolonged bleeding episodes that could otherwise lead to pain, irreversible joint damage, and life-threatening hemorrhages (Coppola et al., 2008; Coppola and Franchini, 2013; Hay, 2007).

With currently marketed FVIII products generally showing circulatory terminal half-lives of 12–14 h in man, prophylactic use typically requires injections every other day or three times weekly, to maintain sufficient circulating levels of FVIII (Bjorkman et al., 2009; Bjorkman and Berntorp, 2001). Various technologies have been used to increase the duration of effect, one being conjugation of therapeutic proteins with water-soluble polymers such as polyethylene glycol (PEG) (Bailon and Won, 2009; Harris and Chess, 2003). Several PEGylated therapeutic proteins are approved for use across a variety of indications, including chronic diseases (e.g., Cimzia®, Mircera®, and PEGASYS® are all protein-based compounds conjugated to 30 or 40 kDa molecular weight [MW] PEGs). The general preclinical and clinical safety aspects of PEGylated products have been reviewed and discussed elsewhere, with the conclusion that no PEG-related safety concerns have been identified at clinically relevant doses of PEGylated products (Ivens et al., 2013; Webster et al., 2007; Webster et al., 2009).

Abbreviations: AUC, area under the concentration-time curve; CL, total plasma clearance; CL_{cl}, intercompartmental distribution clearance; C_0, concentration at time zero; CMP-NAN, cytidine-5′-monophospho-N-acetylneuraminic acid; CNS, central nervous system; EDTA, ethylenediaminetetraacetic acid; ELISA, enzyme-linked immunosorbent assay; FIXa, coagulation Factor FIXa; FVIII, coagulation Factor VIII; FX, coagulation Factor FX; GSC, glycyl sialic acid cytidine monophosphate; HPLC, high-performance liquid chromatography; i.v., intravenous; LRP, low-density lipoprotein receptor-related proteins; LSC, liquid scintillation counting; MW, molecular weight; NCA, noncompartmental analysis; PEG, polyethylene glycol; PK, pharmacokinetics; QWBA, quantitative whole body autoradiography; rFVIII, recombinant coagulation Factor VIII; SA, specific activity; $t_{½}$, terminal elimination half-life; Tris, 2-amino-2-hydroxymethylpropane-1,3-diol; V_c, central distribution compartment; V_p, peripheral distribution compartment; V_{ss}, volume of distribution at steady-state; vWF, von Willebrand factor.

* Corresponding author.
E-mail address: Inbj@novonordisk.com (I. Bjørnsdottir).

http://dx.doi.org/10.1016/j.ejps.2015.10.020

N8-GP, a conjugate of a recombinant FVIII (rFVIII) (turoctocog alfa; NovoEight®) and a single-branched 40 kDa PEG, has been shown to have a good safety profile and improved pharmacokinetics (PK) in hemophilia A patients (Tiede et al., 2013). Site-directed PEGylation and the PEGylation technology in relation to N8-GP conjugate have been described elsewhere (DeFrees et al., 2006; Stennicke et al., 2013).

It has been shown that N8-GP has approximately a 1.5–2-fold longer half-life compared to rFVIII in several species, including the rat (Stennicke et al., 2013) and a hemophilia A dog model (Agerso et al., 2012), as well as in humans (Tiede et al., 2013), with a similar reduction in systemic clearance observed (5.4 versus 9.4 ml/h/kg in the rat for N8-GP and rFVIII, respectively). The prolonged half-life is expected to enable less frequent dosing in humans than for currently used, non-modified rFVIII products.

Stennicke et al. showed that binding of N8-GP to immobilized low-density lipoprotein receptor-related proteins (LRP), an endocytic receptor family abundantly expressed in the liver, was reduced compared to FVIII. As LRP has been implicated with selective clearance of FVIII in the liver (Saenko et al., 1999; Strickland et al., 2014), a protective role of the PEG-moiety in the binding to LRP may likely contribute to the reduced clearance of N8-GP. The same suggested mechanism of prolongation has also been shown for other PEGylated rFVIII (Mei et al., 2010; Turecek et al., 2012). At a molecular weight above 170 kDa, FVIII is not expected to be cleared by the kidneys.

In contrast to the specific clearance pathway of FVIII, PEG molecules in general are predominantly excreted unchanged in the urine by renal filtration, with PEGs of the size used in N8-GP being excreted slowly. Some biliary excretion may occur, likely via hepatocyte and/or Kupffer cell uptake in the liver (Cai et al., 2012; Nesbitt et al., 2009; Webster et al., 2007; Webster et al., 2009; Yamaoka et al., 1994).

The aim of this paper is to describe the biologic fate of [^{3}H]-labeled N8-GP after single i.v. bolus doses to rats, with focus on the fate of the 40 kDa [^{3}H]PEG-moiety. Furthermore, the 40 kDa [^{3}H]PEG-moiety was given separately to rats by single i.v. bolus doses, to investigate whether the PK of [^{3}H]PEG was dose-dependent. For both compounds, the plasma PK, distribution, and elimination were investigated, based on total radioactivity measurements. Finally, the concentration of the intact conjugate was also followed in plasma using an enzyme-linked immunosorbent assay (ELISA) specific to N8-GP.

2. Materials and methods

N8-GP (average MW including the PEG moiety ~219,000 Da) and glycyl sialic acid cytidine monophosphate(GSC) was supplied by Novo Nordisk A/S, Måløv, Denmark. Radiolabeled [^{3}H]PEG and [^{3}H]N8-GP were delivered by Isotope Chemistry at Novo Nordisk A/S. All other solvents and reagents were of analytic grade and purchased from commercial suppliers.

2.1. Synthesis of radiolabeled tracers

[^{3}H]PEG (a) was prepared in a single step from a 40 kDa PEG precursor capped with an allylic moiety (GL2-400 O-allyl-Bz) (b). Tritium was incorporated by saturation of the double bond using tritium gas and a Pd/C catalyst (Fig. 1). High-performance liquid chromatography (HPLC) analysis was applied to establish radiochemical purity, identity, specific radioactivity, and content of residual [^{3}H]40 kDa PEG-Bz.

[^{3}H]N8-GP was synthesized in four steps. In the first step, Allyl-40kPSC (c) was prepared from GL2A-O-allyl-400NP (d) (NOF) and GSC (e) (Malmstrom, 2012), and in the second step, [^{3}H]40 kDa PSC (f) was prepared by saturation of the allyl double bound using tritium gas and Pd/C catalyst (Fig. 1). Then, in the third step, [^{3}H]N8-GP was synthesized by enzymatic conjugation (Stennicke et al., 2013). Turoctocog alfa was desialylated by sialidase to yield free O- and N-glycans, then sialyltransferase (ST3Gal1, supplied by Novo Nordisk A/S) catalyzed the transfer of sialic-acid-[^{3}H]PEG to O-glycan located in the B domain of FVIII. Following the anion-exchange chromatography purification step, the remaining free O- and N-glycans were capped by incubation with ST3Gal3 and cytidine-5′-monophospho-*N*-acetylneuraminic acid (CMP-NAN). The radiochemical purity, identity, and specific activity were analyzed by HPLC, as described below.

2.1.1. Synthesis procedure for [^{3}H]PEG

In a typical reaction mixture GL2-400 O-allyl-Bz (114 mg), MeOH (1 ml), Pd/C 10% (55 mg), tritium gas (466 GBq) was stirred at ambient temperature overnight. To remove Pd/C, the mixture was manually filtered (25 mm Arodish GHP, hydrophilic polypropylene 0.2 μm, Pall Life Science). The crude product was lyophilized three times (3 × 3 ml MeOH) and dissolved in water (3 ml). Basic purification was accomplished by two dialysis steps (Slide-A-Lyzer Dialysis Cassettes 3500 MW, Thermo Scientific, Waltham, MA, USA) against water/sodium chloride (NaCl) (0.1 M, 1000 ml). The yield was 4.4 GBq.

HPLC analysis was conducted on a Dionex ultimate 3000 HPLC system (Thermo Scientific, Waltham, MA, USA) equipped with a Phenomenex Jupiter C18 column, (3 μm, 300 Å, 4.6 × 250 mm), Perkin Elmer Packard 150TR radio-flow detector (PerkinElmer, Waltham, MA, USA), and Shimadzu ELSD-LT-II ELS detector/DAD detector (Holm & Halby, Brøndby, Denmark). The mobile phases consisted of A: milli-Q water and B: MeCN. The system was operated in gradient mode from 10% B to 60% B over 50 min at 35 °C. The radiochemical purity was >95%; however, a broad peak indicated some degree of PEG degradation. The identity was confirmed by HPLC retention time using reference material. The specific activity was crudely estimated to 3 TBq/mmol by HPLC (ELS standard curve versus applied radioactivity), corresponding to roughly three tritium atoms per molecule. The residual content of PEG-Bz was estimated to be <5% by HPLC (UV standard curve versus applied tracer).

2.1.2. Synthesis procedure for [^{3}H]N8-GP

Allyl-40 kDa PSC: GL2A-400 O-allyl-400NP (2.0 g) was dissolved in tetrahydrofuran (THF) (40 ml). This was added to a solution of cytidine monophosphate-5′-Glycyl-neuraminic acid GSC (0.68 g) dissolved in 2-(*N*-morpholino)ethanesulfonic acid buffer (80 ml, 0.5 M pH 8). After 30 min, the THF was removed in vacuo and the product was isolated by five dialysis steps (as above, against water/NaCl 40 ml 0.1 M, 1-h intervals). The material was lyophilized overnight and dissolved/suspended in MeOH (40 ml). After filtration, the product was precipitated by addition of diethyl ether (250 ml) and cooling (5 °C). The precipitate was dried in vacuo (1.8 g) and identity was confirmed by ^{1}H nuclear magnetic resonance spectroscopy in D_2O.

[^{3}H] 40 kDa PSC: Allyl-40 kDa PSC (239 mg) was dissolved in MeOH (1 ml) and Pd/C 10% (50 mg), and tritium gas (529 GBq) was stirred at room temperature for 2 h. The crude product was filtered and lyophilized as described above, and the crude material was dissolved in buffer N (2 ml, 20 mM His, 10 mM $CaCl_2$, 500 mM NaCl, glycerol 20% pH 6.1(His buffer) and used in the following step immediately.

[^{3}H]N8-GP: Turoctocog alfa (2.8 mg/ml) in His buffer (2 ml), sialidase urifaciens (0.4 mg/ml, 50 μl), St3Gal1 (2.5 mg/ml, 250 μl), and [^{3}H]40kDa PSC (25 mg in 250 μl His buffer) were mixed and reacted at ambient temperature for 16–20 h. The sample was diluted with a buffer solution of Tris 25 mM, $CaCl_2$ 5 mM, NaCl 20 mM, glycerol 20%, pH 7.5 (buffer A, 1000 ml), and loaded on a Mono Q 5/50 column (supplied by GE Healthcare, Buckinghamshire, UK). The material was eluted with 0.7 M NaCl in buffer A (buffer B), capped with CMP-NAN and St3Gal3 (CMP-NAN 6 mg in buffer B) and St3Gal3 (1.2 mg/ml, 100 μl), and allowed to react for 0.75 h at ambient temperature. The reaction mixture was purified as described above.

Buffer exchange was performed with L-histidine (1.5 mg/ml), $CaCl_2$ (0.25 mg/ml), Tween 80 (0.1 mg/ml), NaCl (18 mg/ml), sucrose (3 mg/ml), in 1 l H_2O (pH 7) on a size exclusion chromatography using HiLoad 10/600 (supplied by GE Healthcare, Buckinghamshire,

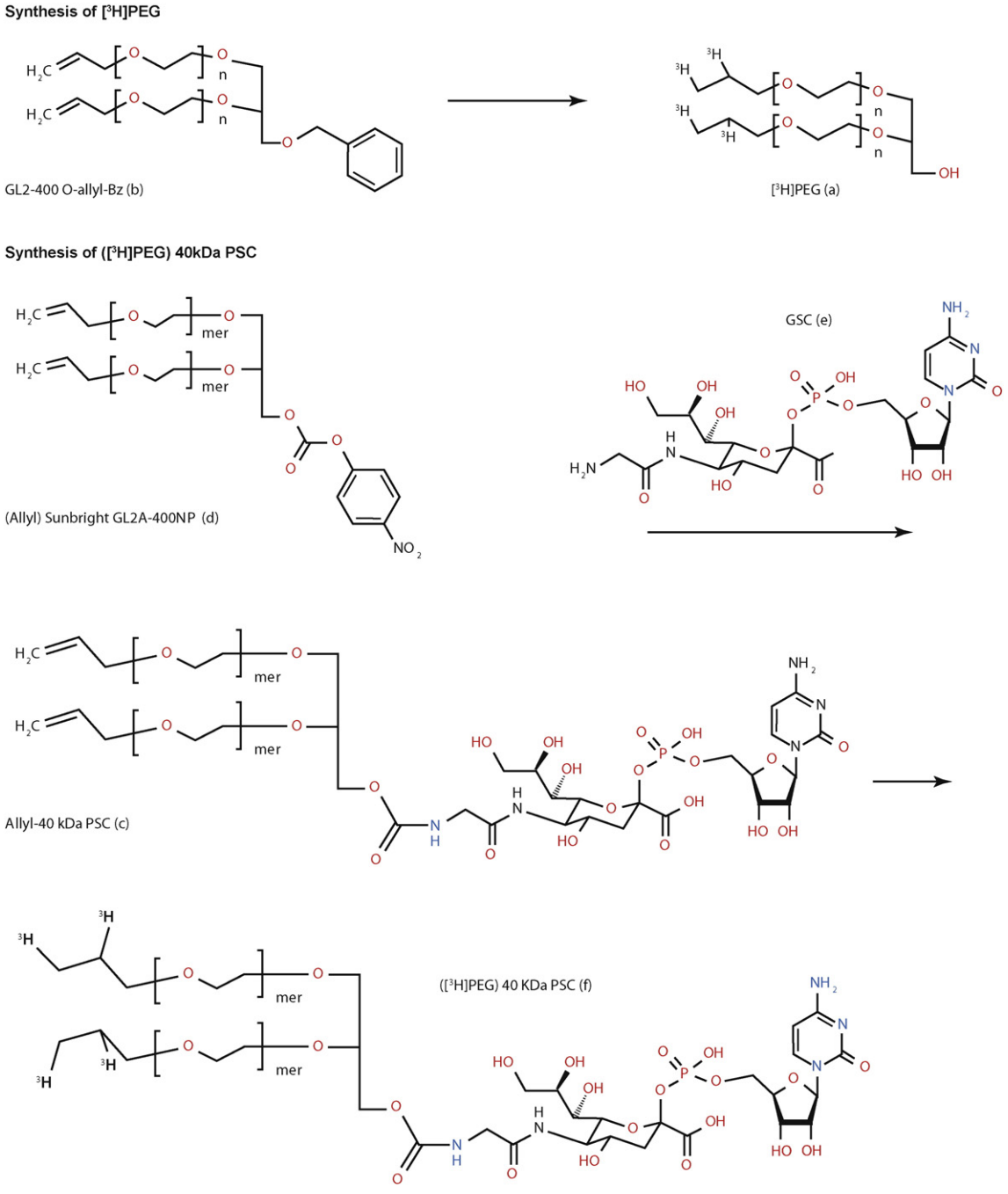

Fig. 1. One-step synthesis of [^{3}H] 40 kDa PEG OH (a) and two-step synthesis of ([^{3}H]PEG) 40 kDa PSC.

UK). HPLC analysis was conducted using a Dionex Ultimate 3000 (as described under synthesis of [^{3}H]PEG) equipped with a Zorbax 300SB C3 column (5 μm, 300 Å 4.6 × 150 mm; Agilent, Santa Clara, CA). The mobile phases consisted of A: 0.1% trifluoroacetic acid in milli-Q water and B: 0.09% trifluoroacetic acid in water:MeCN (20:80). The system was operated in gradient mode from 35% B to 100% B over 50 min at 10 °C, radiochemical purity was >93%, identity was confirmed by HPLC retention time using N8-GP reference material, and the specific activity for [^{3}H]N8-GP was assessed using HPLC – it was found to be between 1.8 and 4.4 TBq/mmol, corresponding to 1.5–4 tritium atoms per molecule.

2.2. In vitro activity of [^{3}H]N8-GP

The quality of the [^{3}H]N8-GP was examined by determination of the specific FVIII activity and by investigating the binding to immobilized von Willebrand factor (vWF). The activity assay measures the cofactor activity of FVIII in FIXa-mediated activation of FX, in the presence of phospholipids and calcium. The reagents from the Coatest SP kit (Chromogenix, Instrumentation Laboratory, Milan, Italy) were used and the assay was carried out as previously described (Stennicke et al., 2013). Dilutions of turoctocog alfa and [^{3}H]N8-GP were analyzed in parallel. Turoctocog alfa, calibrated against the World Health Organisation (WHO) 8th International Standard Factor VIII Concentrate (NIBSC code 07/350), was used as standard in the assay. The FVIII activity per mg protein was calculated by dividing the activity with the protein concentration, which was determined in an ELISA assay and based on two anti-FVIII light chain antibodies (Asserachrom VIIIC:Ag, Diagnostica Stago, France).

The calibrator in the ELISA was turoctocog alfa where the protein concentration was determined by size exclusion chromatography and

by using a batch of turoctocog alfa, for which the protein concentration was determined by amino acid analysis as reference.

The binding to immobilized plasma-derived vWF was determined in an ELISA as described (Christiansen et al., 2010). The bound FVIII was detected using a biotinylated in-house anti-FVIII A2 domain antibody (FVIII-1F5).

2.3. Laboratory animals

All protocols for the in vivo studies were reviewed and approved by the ethical review council at Novo Nordisk A/S prior to study start. The in vivo studies were conducted at Covance under UK home office license and laboratory procedures fully commensurate with international standards of good laboratory practices, but without quality assurance assessment. Male Han Wistar rats (HsdHanTM, WIST), with an initial weight between 190 and 257 g (7–9 weeks of age) were used in all studies. Most rats were obtained from Harlan, Blackthorn, UK but rats used in the tissue distribution study of PEG were delivered by Charles River UK Ltd. (Margate, UK) due to constraints in delivery of rats of the right age and size from Harlan at the time this study was conducted.

All rats were housed up to five per cage, in solid floor cages containing suitable bedding. Rats were single housed when they were in the metabolism cages for collection of excreta, and were rehoused in groups in the time intervals between the collection periods. The rats were kept in rooms thermostatically maintained at a temperature of 18–24 °C, with a relative humidity of between 45 and 79% and exposed to fluorescent light in 12-h cycles. Temperature and relative humidity were recorded on a daily basis. The facility was designed to give 15–20 air-changes per hour.

The rats were provided with wooden Aspen chew blocks and polycarbonate tunnels in order to enrich both the environment and the welfare of the animals. Though they were not given chew blocks or tunnels when in glass metabolism cages, they were provided with glass hoops as an alternative form of environmental enrichment. For the animals not housed in metabolism cages, the bedding, chew blocks and tunnels were replaced at the end of the working day on dose day and again at the end of the next working day. This was done in order to reduce the potential for contamination and further ingestion of drug-related material. The rats were allowed free access to commercial pellet diet and water at all times during the study.

2.4. Experimental design

2.4.1. Excretion recovery and plasma sampling

Male Han Wistar albino rats ($n = 3$) were dosed with a single intravenous dose of either [^{3}H]N8-GP (low dose: 0.17 mg/kg, ~1160 U/kg at an activity of 8500 U/mg, PEG load of ~0.03 mg/kg; high dose: 4.1 mg/kg, ~28,000 U/kg, PEG load of ~0.7 mg/kg) or 40 kDa [^{3}H]PEG (1, 12, 100, or 200 mg/kg). It should be noted that the exact concentration in U/kg for the highest dose of [^{3}H]N8-GP is unknown since the in vitro activity was only tested for the lower dose formulation. The corresponding doses in radioactivity were: 3.5 and 35 MBq/kg respectively for the two doses of [^{3}H]N8-GP and 30–37 MBq/kg for [^{3}H]PEG. All [^{3}H]N8-GP dosed rats were given higher doses than given therapeutically to humans (50–75 U/kg, ~PEG load of <0.002 mg/kg). This was done in order to secure reliable detection of radioactivity for up to 12 weeks post-dosing. The rats were kept in standard glass metabolism cages continuously for the first 3 days of the study period and thereafter for 24-h intervals on a weekly basis up to 12 weeks.

The samples were prepared in various ways prior to measuring the total radioactivity using liquid scintillation counting (LSC). Volumes and/or weights of biologic samples were measured where appropriate. Plasma, urine, and cage washings were added directly to liquid scintillant prior to LSC. Feces and cage debris were homogenized in an appropriate volume of deionized water and then solubilized using a suitable volume of solubilizing agent (Soluene®-350; PerkinElmer LAS [Beaconsfield, UK]). After an appropriate period of incubation, liquid scintillant was added and the samples measured by LSC. Carcasses were digested in a solution of potassium hydroxide in methanol (approximately 40%, weight per volume) and then measured by LSC. Recoveries of radioactivity were calculated over time and the total recovery of the administered dose was estimated by interpolation between the sampling points.

Blood was collected from 5 min up to 12 weeks post-dose at all dose levels, from the jugular vein. A total of 12 rats (2×6 rats) were used for collection of blood for each compound and dose, with 6 rats sampled at 5 min; 1, 6, and 24 h; and 1, 3, 5, 7, 9, and 11 weeks post-dose, and 6 rats sampled at 30 min; 2, 8, and 48 h; and 2, 4, 6, 8, 10, and 12 weeks post-dose. Blood samples were then pooled per time point.

For [^{3}H]N8-GP, for the first 4 weeks following dosing, blood samples were split in two immediately after withdrawal. One part was collected in a tube containing tri-sodium citrate as anticoagulant to provide a pooled blood sample per time point from six animals, with a minimum of 100 μl plasma needed for exploratory ELISA. The remainder of the blood sample was collected in a tube containing EDTA as anticoagulant and subsequent centrifugation (4000 *g*, 10 min, 20 °C) to provide a pooled plasma sample per time point from six animals for provision of plasma for LSC analysis. Pooled plasma samples from [^{3}H]PEG dosed rats were also obtained using EDTA as anticoagulant and subsequent centrifugation. Plasma samples from both [^{3}H]PEG- and [^{3}H]N8-GP-dosed rats were analyzed in duplicate to obtain total radioactivity count data using LSC.

2.4.2. Tissue distribution

For the quantitative whole body autoradiography (QWBA) studies, male Han Wistar albino rats ($n = 9$) were dosed with a single i.v. dose of either 4.1 mg/kg [^{3}H]N8-GP (35 MBq/kg, ~28,000 U/kg, PEG load of ~0.7 mg/kg) or 0.6 mg/kg [^{3}H]PEG (37 MBq/kg).

Following anesthesia under isoflurane, one rat per time point was sacrificed by a 30-min cold shock (plunged into a freezing mixture of excess of solid CO_2 in hexane). Once fully frozen, the carcasses were prepared for analysis using the QWBA techniques. The sampling time points were 1, 12, 24, and 96 h, and 1, 2, 5, 9, and 12 weeks post-dose.

Immediately prior to sacrifice, a blood sample was taken from each animal by cardiac puncture and collected into EDTA-precoated tubes; samples were then centrifuged to obtain plasma (4000 *g*, 10 min, 20 °C).

2.4.3. In vivo stability of [^{3}H]PEG and [^{3}H]N8-GP

Plasma samples obtained in relation to the two tissue distribution studies were divided into two aliquots prior to LSC. One aliquot was analyzed directly by LSC, the other was freeze-dried, reconstituted in water and analyzed by LSC to enable the quantification of the volatile tritiated water content in the original sample.

2.4.4. ELISA assay for detection of N8-GP in rat plasma

The sandwich ELISA used to quantify intact N8-GP utilized two detection antibodies. One antibody was directed against an epitope on the PEG-moiety and the other against an epitope on FVIII. In brief, microtiter plates were coated with an anti-PEG antibody (LAGH-2F8) and free binding sites were blocked using buffer containing 1% bovine serum albumin and 0.05% Tween 20. Prediluted calibrators and samples were further diluted 1:5 in rat EDTA plasma, and added to the coated plates together with a HRP conjugated detection antibody directed against FVIII (BDD-FVIII-1F10). After washing of the plates, a peroxidase substrate buffer was added; this contained a chromogenic reagent, Tetramethylbenzidine (3,3′,5,5′-Tetramethylbenzidine), allowing for quantification of N8-GP conjugate present in the samples.

2.5. Pharmacokinetic analysis

Plasma radioactivity concentration versus time data from the excretion balance and the QWBA studies were used to assess the distribution

and elimination kinetics of total plasma radioactivity stemming from single i.v. doses of [^{3}H]PEG or [^{3}H]N8-GP. The radioactive concentrations were transformed to nmol equivalents/g plasma using the specific activity of the respective radioactive formulations (simplified to nmol/l or nM throughout this paper).

Due to the unspecificity of using total radioactivity measurements, challenges in interpreting the resulting pharmacokinetic (PK) parameters exist. It is for example not a certainty that the PK analysis of plasma radioactivity from [^{3}H]PEG-dosing solely represents the intact 40 kDa PEG as the results may represent the kinetics of a mixture of intact PEG and any metabolites formed over the sampling period. However, as a 40 kDa PEG is generally considered to be a metabolically stable compound ((Webster et al., 2007); see also 'the discussion'), it is deemed likely that the majority of plasma radioactivity measured in this study after i.v. dosing of [^{3}H]PEG can be attributed to the intact 40 kDa PEG.

Assessment of [^{3}H]N8-GP-related plasma radioactivity is further complicated by the fact that the compound is a conjugate of two entities with vastly different kinetics, meaning that the measured plasma radioactivity is likely to represent different ratios of intact [^{3}H]N8-GP and [^{3}H]PEG, or any metabolites, at different time points.

For the reasons described above, the PK evaluation of plasma radioactivity should be interpreted with some caution. However, for the purposes of this study it was still deemed useful to describe the disposition of the total radioactive dose quantitatively to be able to make some simple comparisons between different dose levels of [^{3}H]PEG and between [^{3}H]PEG- and [^{3}H]N8-GP-related plasma radioactivity.

To assess the kinetics of the intact N8-GP conjugate after [^{3}H]N8-GP i.v. dosing, plasma concentrations from ELISA measurements were used.

As the blood samples were collected in a sparse sampling design, mean composite plasma profiles were produced from pooled samples ("naïve pool method"; $n = 6$/time point) for each compound and dose level prior to noncompartmental analysis (NCA). The PK parameters assessed by NCA were the back-extrapolated concentration at time zero (C_0), terminal elimination half-life ($t_{½}$) (based on linear regression of the log-linear terminal phase), mean residence time (MRT), total plasma clearance (CL), volume of distribution at steady-state (V_{ss}), and the areas under the concentration-time curves from time zero to time t ($AUC_{(0-t)}$), and from zero to infinity (AUC). The extrapolated area (AUC_{extrap}) from the last sampling time point to infinity was also estimated.

To further assess the observed dose-dependency in the kinetics of the total plasma radioactivity after various i.v. dose levels of [^{3}H]PEG, a standard open 2-compartment i.v. bolus first-order elimination model was explored. Here, the volumes of the central and peripheral distribution compartments (V_c and V_p), the inter-compartment distribution clearance (CL_d) and CL were estimated. A proportional error model was used for fitting the model to the plasma concentration data.

All PK analyses were performed in Phoenix™ WinNonlin® version 6.2 (Pharsight, St. Louis, MI).

3. Results

3.1. In vitro activity of [^{3}H]N8-GP

The FVIII activity of [^{3}H]N8-GP was 8500 U/mg, close to the value obtained for the N8-GP starting material (i.e., 11,000 U/mg), indicating that [^{3}H]N8-GP had retained close to full FVIII in vitro activity (~80%). [^{3}H]N8-GP showed retained capability of binding to vWF as the binding affinity of [^{3}H]N8-GP to vWF was similar for [^{3}H]N8-GP and turoctocog alfa.

3.2. In vivo stability of [^{3}H]PEG and [^{3}H]N8-GP

To assess any potential in vivo stability issue, [^{3}H]PEG and [^{3}H]N8-GP tracers were evaluated via determination of the amount of ^3H_2O in plasma samples. None to very low amounts of tritiated water in plasma were generated for both tracers up to 12 weeks post-dose.

3.3. Tissue distribution of [^{3}H]PEG

The tissue distribution of [^{3}H]PEG after i.v. administration was followed for up to 12 weeks post-dose. Radioactivity was widely distributed, mainly in the highly vascularized tissues, and was gradually eliminated (Fig. 2A).

Peak concentrations of radioactivity typically occurred at 1 or 12 h post-dose (first and second sample), with more than nine out of ten investigated tissues containing peak concentrations of radioactivity at these time points. Tissues containing the highest levels of radioactivity were, in order of magnitude: urine, blood, lungs, bile ducts, lymph, adrenal glands, and kidneys. Radioactivity was detectable in the majority of tissues up to 5 weeks post-dose and at the final sampling time point (week 12) radioactivity was still widely distributed, with approximately one-third of the tissues still containing low levels of quantifiable radioactivity. The tissues in the central nervous system (CNS) (brain and spinal cord) were exposed to low levels of drug-related material and only quantifiable at the two earliest time points after dose administration (1 and 12 h).

3.4. Tissue distribution of [^{3}H]N8-GP

The radioactivity in rat tissues after i.v. administration of [^{3}H]N8-GP was widely distributed and gradually eliminated (Fig. 2B). Radioactivity was distributed at low levels throughout the whole body into more than 50 tissues in the male rat. Peak concentrations of radioactivity typically occurred at the 1-, 12-, and 24-h sampling times, with about 75% of the investigated tissues containing peak concentrations of radioactivity at these times. The highest levels of radioactivity were found in highly vascularized tissue/organs, with the highest levels of radioactivity detected in (in order of magnitude): plasma, blood, lymph, liver, spleen, bile ducts, lungs, kidneys, and adrenal glands. Approximately half of the tissues contained quantifiable levels of radioactivity at the final sampling time (12 weeks), with the highest amounts in lymph, liver, and spleen. Low levels of radioactivity (close to the detection limit) were present in the CNS (brain and spinal cord) at all time points, with the last data point measured at 5 weeks post-dose.

3.5. Excretion of [^{3}H]PEG

The estimated total recoveries for the four excretion studies performed with [^{3}H]PEG were between 88 and 93% (Table 1). [^{3}H]PEG-related radioactivity was excreted in both urine and feces, with urinary excretion as the major route of elimination (75%, 73%, 56%, and 62% excreted in urine 12 weeks post-dose for the 1 mg/kg, 12 mg/kg, 100 mg/kg, and 200 mg/kg, respectively). The fraction excreted in feces was similar for all four dose levels (~10% of the radioactive dose). In contrast, the lower doses of [^{3}H]PEG seemed to provide increasing fractions excreted in urine (Table 1; Fig. 3). The majority of radioactivity (>50%) of each of the four doses was excreted within 1 week post-dose but some radioactivity still remained to be excreted at the last time point (5–20%; 12 weeks post-dose). The fraction that remained in the carcass after 12 weeks seemed to be dependent on dose – it was higher with increasing dose. Low levels of radioactivity were still being excreted at the final time point (0.05–0.1% per day).

3.6. Excretion of [^{3}H]N8-GP

The average interpolated excretion recovery for [^{3}H]N8-GP was found to be 78% for the 4.1 mg/kg dose and 104% for the 0.17 mg/kg dose (see Table 1). The reason for the difference in total recovery is unknown. PEG-related radioactivity was excreted both in urine and in feces, though the percent of dose excreted in the urine at the low dose

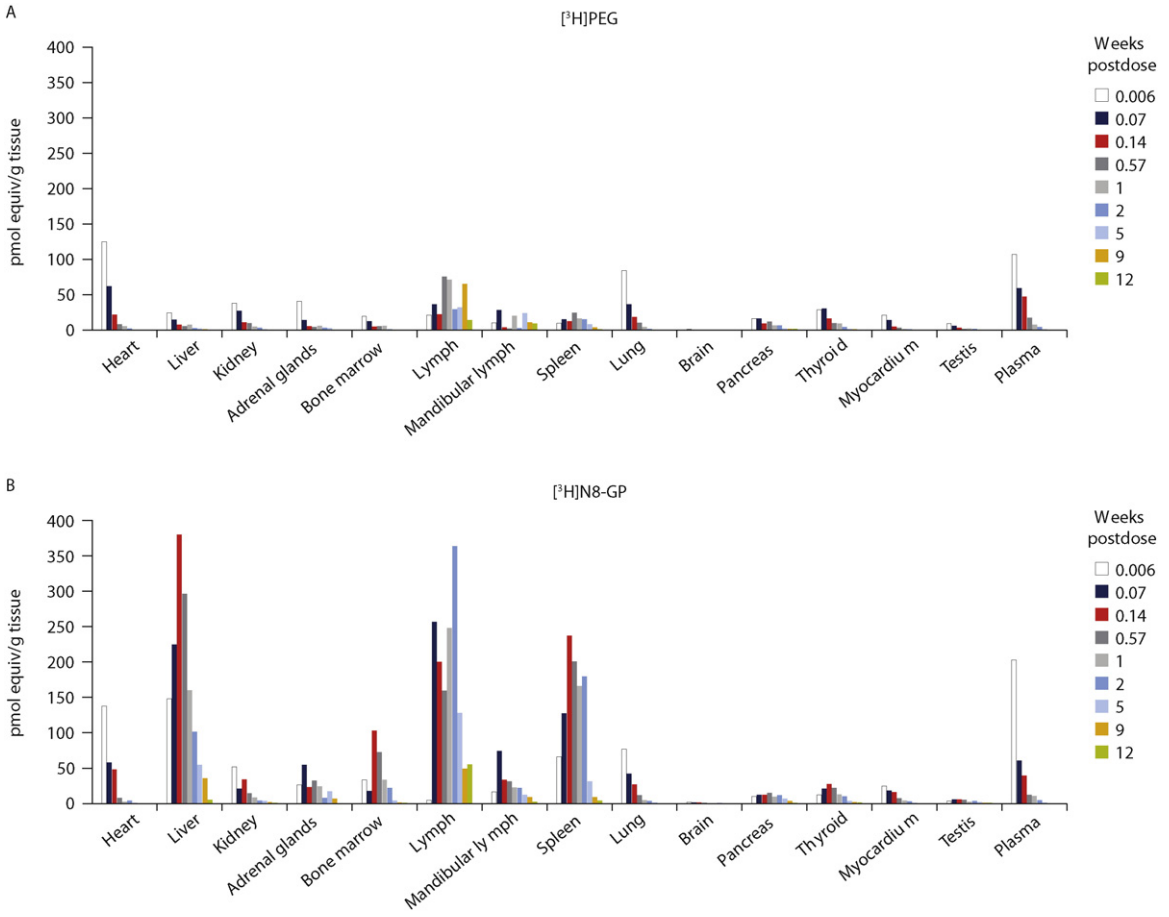

Fig. 2. Tissue/organ distribution of radioactivity related to [^{3}H]PEG (A) or [^{3}H]N8-GP (B) at 1, 12, 24, and 96 h, and 1, 2, 5, 9 and 12 weeks post-dose after a single intravenous administration at a dose of 0.6 mg/kg [^{3}H]PEG and 4.1 mg/kg [^{3}H]N8-GP (~PEG load of 0.7 mg/kg) in Wistar rats ($n = 1$ per time point).

(63%) was much higher than for the high dose (34%). The percent of dose excreted in feces was similar at the two dose levels (~35%). Furthermore, in total, approximately 50% of the radioactive dose was excreted during the first 1 or 2 weeks post-dosing. Only a small amount of radioactivity remained to be excreted at the final time point of 12 weeks post-dose (5.6% and 7.7% for the 0.17 mg/kg and 4.1 mg/kg doses, respectively). PEG-related radioactivity was still being excreted at a low rate (~0.2% per day) at this time.

3.7. Pharmacokinetics after i.v. dosing of [^{3}H]PEG

The PK of [^{3}H]PEG-related plasma radioactivity was investigated in the rat after single i.v. bolus administration of 0.6, 1, 12, 100, and 200 mg/kg [^{3}H]PEG. The evaluation was based on total radioactivity measurements converted to nmol equivalents per liter. As discussed above, the PK evaluation was interpreted with the assumption that the total plasma radioactivity after dosing of 40 kDa [^{3}H]PEG is mainly attributed to the intact molecule throughout the study; the PK evaluation should be interpreted with this in mind.

The mean composite plasma profiles of total radioactivity from the different [^{3}H]PEG dose levels are shown on a semi-logarithmic scale in Fig. 4a. The profiles appeared to display a biphasic decay after i.v. dosing at all five dose levels, with an initial decline in concentrations over the first 1 or 2 weeks, where after a slower terminal phase was observed until the end of the experiment 12 weeks post-dose. At week 12, detectable levels of radioactivity were still present in plasma for all dose levels.

Though the most obvious difference between the plasma concentration versus time profiles was seen for the lowest [^{3}H]PEG dose of 0.6 mg/kg compared to the higher dose levels (especially from dose-normalized data; Fig. 4b), possibly caused by a higher clearance of radioactivity after the 0.6 mg/kg dose, there was also evidence of a slower terminal elimination phase after the 100 and 200 mg/kg doses versus the 1 and 12 mg/kg doses. Notably, even though substantially longer terminal $t_{½}$ for the plasma radioactivity were estimated after the two highest dose levels (42–59 days) compared to the two lower

Table 1
Estimated excretion recoveries (%) following single intravenous bolus doses of [^{3}H]PEG or [^{3}H]N8-GP.

[^{3}H]PEG (% of dose)					[^{3}H]N8-GP (% of dose)	
	200 mg/kg	100 mg/kg	12 mg/kg	1 mg/kg	4.1 mg/kg N8-GP ~0.7 mg/kg PEG	0.17 mg/kg N8-GP ~0.03 mg/kg PEG
Urine[a]	62.4	55.5	73.3	74.8	34.4	62.7
Feces	12.0	12.4	13.4	12.6	37.5	33.4
Carcass	18.2	20.3	6.1	5.4	5.6	7.4
Total	92.6	88.2	92.8	92.8	77.5	104

[a] Cage wash is included in urine.

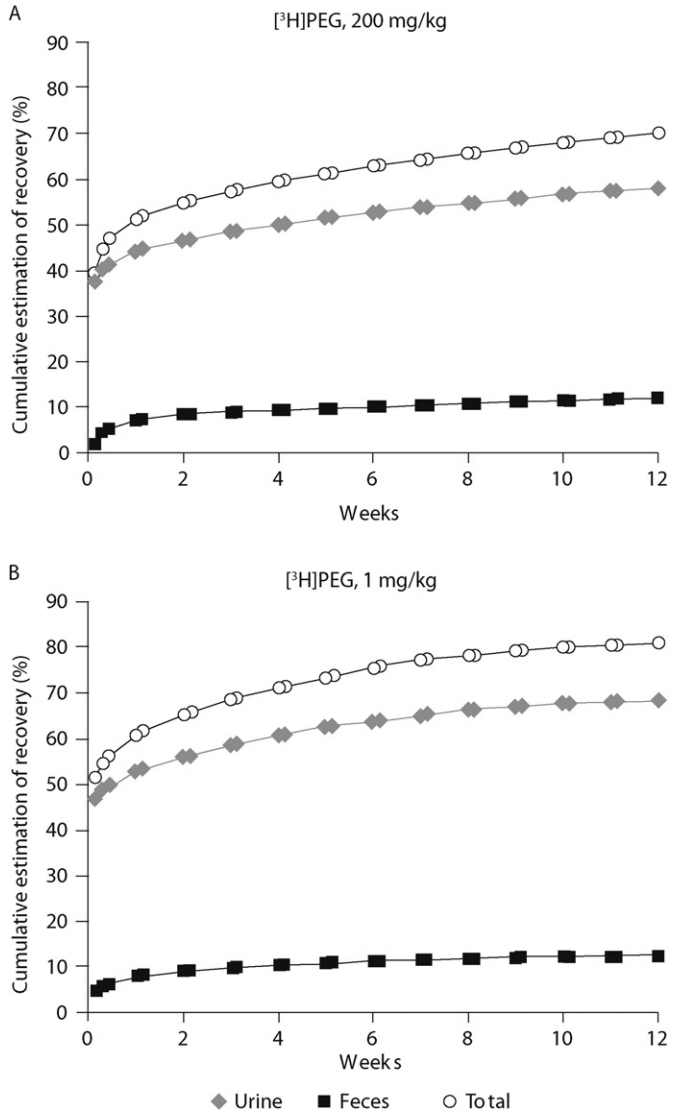

Fig. 3. Cumulative excretion results of radioactivity for the highest (200 mg/kg) and lowest (1 mg/kg) dose of [^{3}H]PEG ($n = 3$ per time point).

dose levels (24–26 days), total AUC generally increased in a dose-proportional manner between 1 and 200 mg/kg. Though the latter may not appear to align with a dose-dependent terminal $t_{½}$, a likely explanation can be found in the fact that a large fraction of the radioactive dose had already been eliminated before the start of the terminal phase (40–60% after 1 week; Fig. 3). This means that a major fraction of the total AUC was not affected by the different terminal rates. For the 0.6 mg/kg [^{3}H]PEG dose, the terminal $t_{½}$ of radioactivity was estimated to be 19 days.

From NCA analysis, the plasma clearance of [^{3}H]PEG-related radioactivity appeared to be similar for doses between 1 and 200 mg/kg, while the apparent distribution volume of the radioactivity (V_{ss}) was approximately 2-fold higher after the two highest doses (Table 2). This was also confirmed by fitting a standard 2-compartment model to the data, which further indicated that the nonlinearity of the total plasma radioactivity seen for the two highest dose levels was due to a difference in the peripheral distribution volumes. Because of the apparent nonlinearity observed for [^{3}H]PEG-related radioactivity, one set of parameter estimates could not adequately explain plasma data from all dose levels simultaneously in the standard 2-compartment model. For the scope of the current assessment, being able to compare model parameters across dose levels was deemed sufficient, hence more sophisticated models were not explored and the dose levels were modeled individually. The actual model fit of the data is shown in Fig. 5 and the model parameter estimates are listed in Table 3.

From the model fit of the plasma radioactivity data, estimation of total CL and total apparent volume of distribution produced similar results as the NCA (Table 3). The peripheral volume of distribution (V_p) for the [^{3}H]PEG-related plasma radioactivity was much larger than the central volume (V_c). For the two highest dose levels, the modeling results indicated that an increase in V_p was responsible for the total increase in the apparent volume of distribution and hence likely the longer terminal $t_{½}$ observed at these dose levels compared to the 1 and 12 mg/kg doses.

There was approximately a 2-fold difference in the estimated V_c after the 0.6 mg/kg dose level. This is likely an effect of the different sampling schedule used at this dose level, where fewer early blood samples were collected after dosing compared to the other dose levels.

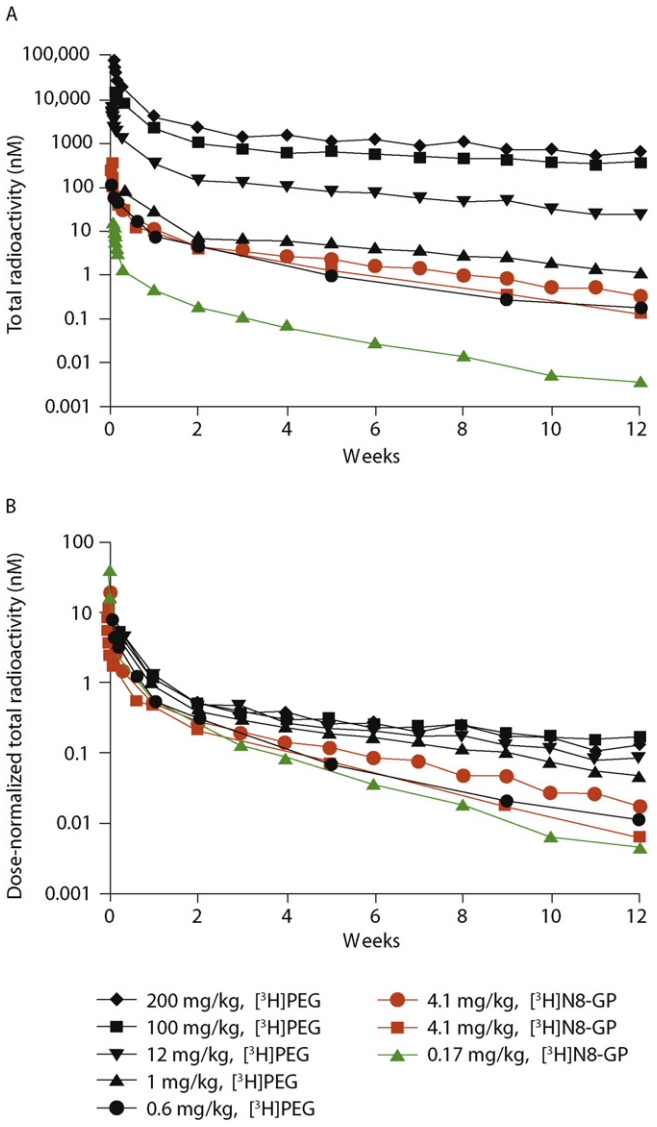

Fig. 4. Total plasma radioactivity concentrations, converted to nmol equivalents/l (or nM), for single intravenous bolus doses to rats of 0.6, 1, 12, 100, and 200 mg/kg [^{3}H]PEG or 0.17 and 4.1 mg/kg [^{3}H]N8-GP. (A) Semi-log plot; (B) semi-log plot of dose-normalized data ($n = 6$ rats per time point, except for the 0.6 mg/kg dose of [^{3}H]PEG and one of the two 4.1 mg/kg doses of [^{3}H]N8-GP (red squares) where $n = 1$ per time point). Data from the two 4.1 mg/kg [^{3}H]N8-GP studies originate from two separate studies: tissue distribution (red squares) and excretion/plasma sampling (red circles).

Table 2
PK parameter estimates from noncompartmental analysis of total plasma radioactivity after single intravenous bolus doses of 0.6, 1, 12, 100, or 200 mg/kg [^{3}H]PEG or 0.17 and 4.1 mg/kg [^{3}H]N8-GP and plasma concentrations of N8-GP after 0.17 and 4.1 mg/kg [^{3}H]N8-GP.

Parameter/dosed compound (assay)	[^{3}H]PEG (LSC)					[^{3}H]N8-GP (LSC)			N8-GP (ELISA)	
Dose (mg/kg)	0.6	1	12	100	200	0.17	4.1[a]	4.1[b]	0.17	4.1[b]
C_0 (nM)	114	477	5260	38,900	83,800	35.6	207	413	68.4	375
$AUC_{(0\text{-}1wk)}$ (h*nM)	4650	13,500	190,000	1,350,000	2,650,000	331	4190	5160	148	1710
AUC (h*nM)	7340	22,900	360,000	3,180,000	5,750,000	449	7250	9550	148	1710
AUC/dose ((h*nM)/(nmol/kg))	524	996	1290	1380	1220	569	370	487	188	87.3
AUC_{extrap} (%)	1.3	4.4	5.6	21	14	0.31	0.84	2.5	0.14	0.53
CL (ml/h/kg)	1.9	1.0	0.78	0.72	0.82	1.8	2.7	2.1	5.32	11.4
V_{ss} (ml/kg)	500	430	390	870	690	300	770	790	50.6	103
$t_{½}$ (days)	19	24	26	59	42	13	14	19	0.2	0.27
MRT (days)	11	18	21	50	35	7.0	12	16	0.40	0.38

[a]QWBA study. [b]Excretion balance study. MRT, mean residence time.
Note: sparse sampling design with each sample representing pooled concentrations from 6 rats.

This can also be seen from calculating the initial volume of distribution of the dosed radioactivity from NCA data in Table 2 (dose/C_0), where V_0 is approximately the size of plasma volume for the doses between 1 and 200 mg/kg, but approximately 2-fold higher for the 0.6 mg/kg. This difference in V_0 is likely caused by an underestimation of the back-extrapolated C_0 due to the described lack of early samples for this dose level.

The fraction of the administered [^{3}H]PEG dose remaining to be eliminated from plasma after 12 weeks increased with increasing dose and was estimated to be approximately 1% for the 0.6 mg/kg dose, 4–6% for the 1 and 12 mg/kg doses, and 21% and 14% for the 100 and 200 mg/kg doses (AUC_{extrap}; Table 2).

3.8. Pharmacokinetics of [^{3}H]N8-GP-related radioactivity in plasma

The plasma PK of N8-GP was investigated in the rat after single i.v. bolus administration of 0.17 and 4.1 mg/kg [^{3}H]N8-GP (~1300 and 30,000 U/kg). The evaluation was based on total radioactivity measurements or ELISA concentration measurements of the intact conjugate, both converted to nmol/l. As discussed earlier the total radioactivity measurements may represent intact [^{3}H]N8-GP, [^{3}H]PEG or various radioactive metabolites, with the ratios of these varying over time, the PK evaluation should be interpreted with this in mind.

The mean composite plasma radioactivity profiles from the two different dose levels are shown on a semi-logarithmic scale in Fig. 4.

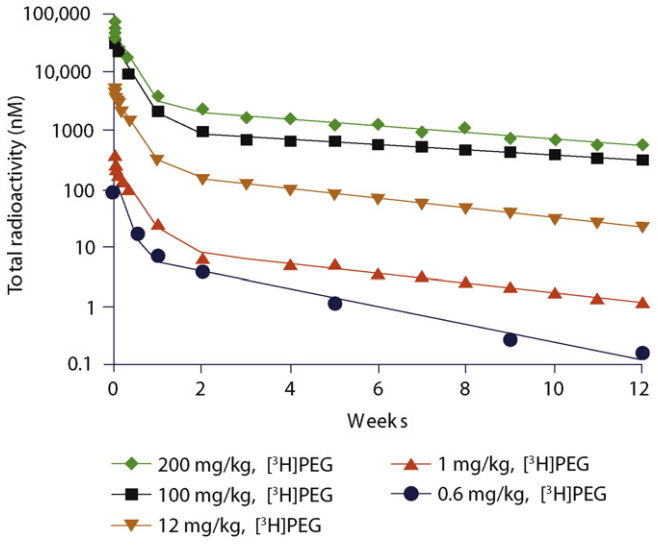

Fig. 5. Model fit to [^{3}H]PEG-related plasma radioactivity data. A standard 2-compartment model with linear elimination was used. Due to potential nonlinearity after [^{3}H]PEG i.v. dosing, individual fits per dose were performed ($n = 6$ rats per time point, except for the 0.6 mg/kg dose where $n = 1$ per time point).

As observed for [^{3}H]PEG, the radioactivity profiles collected after i.v. dosing of [^{3}H]N8-GP appeared to display a biphasic decay in plasma concentrations, with a relatively rapid decline in concentrations during the first week post-dose and a subsequent much slower terminal elimination phase-out to 12 weeks post-dose.

In Fig. 6, the plasma concentration versus time profiles of the N8-GP conjugate (as measured by ELISA) are plotted together with the total radioactivity profiles after dosing of [^{3}H]N8-GP. To better visualize the ELISA data, only the first 14 days post-dose are displayed. It is apparent that N8-GP exists in plasma as an intact conjugate for up to a few days following dosing. This is much shorter than that observed for [^{3}H]PEG-related radioactivity after dosing of [^{3}H]N8-GP. Plasma clearance was higher, and a lower apparent distribution volume was estimated by NCA for the conjugate compared to that for total radioactivity (Table 2), with a terminal $t_{½}$ for the former estimated to approximately 5–6 h.

Plasma clearance of total radioactivity appeared to be similar for the two investigated dose levels; however, the estimated apparent V_{ss} was almost 2-fold larger following the higher dose (Table 2). The terminal $t_{½}$ of plasma radioactivity was 13 days for the 0.17 mg/kg dose and 14–19 days for the 4.1 mg/kg doses. Furthermore, the fraction of the administered radioactive dose remaining to be eliminated from plasma 12 weeks post-dose was estimated to be approximately 0.3% for the 0.17 mg/kg dose and 0.8–2.5% for the 4.1 mg/kg doses (AUC_{extrap}; Table 2).

Similarly after [^{3}H]PEG dosing, a large fraction of the administered [^{3}H]N8-GP-related radioactivity was already eliminated from plasma after the first week of dosing (>70% after 0.17 mg/kg and 50–60% after 4.1 mg/kg) (Table 2).

4. Discussion

The distribution and elimination of a novel PEGylated rFVIII (N8-GP) were assessed in rats over 12 weeks after single i.v. administration of [^{3}H]N8-GP. Single doses of the 40 kDa [^{3}H]PEG were also assessed.

Table 3
Estimated model parameters after fitting a 2-compartment model to total concentrations of plasma radioactivity after single intravenous bolus doses of 0.6, 1, 12, 100, or 200 mg/kg [^{3}H]PEG.

Parameter	[^{3}H]PEG				
Dose (mg/kg)	0.6	1	12	100	200
V_c (ml/kg)	160 (12)	90 (7.5)	81 (5.2)	85 (5.3)	84 (6.6)
V_p (ml/kg)	360 (14)	310 (15)	310 (9.8)	670 (12)	580 (13)
V_{tot} (ml/kg)	520 (11)	400 (12)	390 (8.1)	760 (11)	670 (11)
CL (ml/h/kg)	1.9 (6.7)	1.0 (6.0)	0.82 (4.2)	0.78 (4.9)	0.89 (5.7)
CL_d (ml/h/kg)	1.2 (25)	0.57 (18)	0.68 (15)	0.85 (12)	1.0 (18)

[a]QWBA study.
[b]Excretion balance-study.
CV% is stated within brackets.

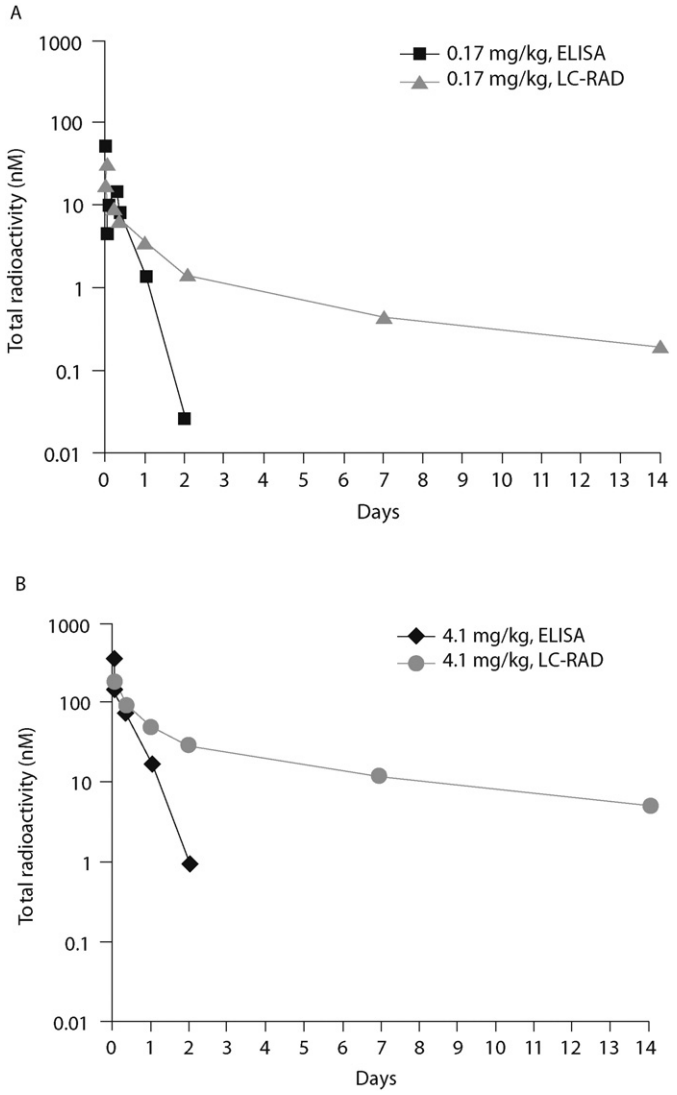

Fig. 6. Plasma concentrations of total radioactivity (gray triangles and circles) and plasma concentrations of intact N8-GP (black squares and diamonds) versus time after single intravenous bolus doses of 0.17 (A) or 4.1 mg/kg [^{3}H]N8-GP (B) to the rat. Radioactive concentrations were converted to nM. It should be noted that only the first 14 days post-dose are shown to enable better visualization of the ELISA data ($n = 6$ per time point for all studies).

The optimal position of an isotope label in N8-GP to appropriately characterize the ADME properties of the PEG-moiety was assessed at an early stage and resulted in labeling of the PEG-moiety. Labeling the protein backbone was also considered but would have resulted in a plasma concentration-time profile resembling the ELISA data of N8-GP (Fig. 6), and any PK assessment of such data would describe the fate of intact N8-GP and metabolites, rather than the PEG.

Radiolabeling with tritium was selected in favor of carbon-14, based on a combination of higher specific radioactivity and a wish to use traditional analytic techniques (e.g., QWBA and LSC). In contrast to simple tritium exchange of labile hydrogen atoms, the current ^{3}H-labeling was based on specific and stable aliphatic labeling in the propylic capping group at the end of each PEG chain. The ^{3}H-labeling of the PEG was found to be stable and fit-for-purpose as very little, or no, tritiated water was detected in plasma samples throughout the studies, thus allowing meaningful assessment of the fate of both [^{3}H]N8-GP and [^{3}H]PEG.

Previous findings of the plasma kinetics of the intact N8-GP conjugate in rats (Stennicke et al., 2013) were confirmed in these studies, with an N8-GP plasma $t_{½}$ of 5–6 h, representing the removal and/or metabolism of intact N8-GP.

The plasma profiles of total radioactivity appeared to be biphasic in nature, both after i.v. dosing of [^{3}H]N8-GP and [^{3}H]PEG. Plasma clearance of [^{3}H]PEG-related radioactivity was higher after dosing of [^{3}H]N8-GP compared to after dosing of [^{3}H]PEG. Apparent volume of distribution of radioactivity was fairly large after dosing of either compound, especially after the higher doses.

Using a simple 2-compartment PK model to describe the plasma radioactivity after i.v. dosing of [^{3}H]PEG, radioactive material appeared to be relatively widely distributed to the periphery as seen by a large estimated V_p. Further, total clearance and distribution clearance of plasma radioactivity were generally of similar magnitude, indicating that these were competing processes. Consequently, a substantial fraction of the radioactive dose would be expected to be cleared before distribution equilibrium. This was also confirmed by excretion data, which indicated that at least half of the radioactivity dosed was eliminated 1–2 weeks post-dose. This latter finding was also true for radioactivity related to [^{3}H]N8-GP dosing. QWBA data showed a wide distribution of radioactive material for both compounds, particularly to the highly vascularized tissues, with a gradual decrease in radioactivity over time.

After distribution equilibrium was reached for plasma radioactivity around one ([^{3}H]N8-GP) or two ([^{3}H]PEG) weeks post-dose, a slow terminal elimination phase was apparent. This pattern has also been observed for other PEGylated compounds such as certolizumab pegol, a 40 kDa PEG conjugated to a Fab' (Nesbitt et al., 2009). Judging by the faster rate of disappearance from plasma of the N8-GP conjugate (as measured by ELISA) and the similar terminal phases of plasma radioactivity when [^{3}H]N8-GP or [^{3}H]PEG were dosed at similar PEG-loads, the slow elimination phase is likely due to [^{3}H]PEG-related material. This would indicate that the 40 kDa PEG-moiety behaves kinetically similar after detachment from the rFVIII-moiety as when dosed alone.

In general, the protein part of PEGylated proteins is thought to be degraded via proteolysis to short peptides and amino acids by lysosomal enzymes. The PEG and/or PEG and linker are then supposedly released to the lymphatics and blood (Baumann et al., 2014; Elliott et al., 2012; Webster et al., 2009). FVIII is believed to be selectively cleared in the liver via the LRP pathway (Bovenschen et al., 2003; Saenko et al., 1999; Strickland et al., 2014), but PEGylation of rFVIII has been shown to delay this interaction, resulting in prolongation of the plasma $t_{½}$ (Stennicke et al., 2013). PEG is likely also cleared via the LRP pathway when still attached to rFVIII, as evidenced by the larger fraction of radioactivity collected in the feces for [^{3}H]N8-GP versus [^{3}H]PEG (30% vs. 10%).

[^{3}H]PEG-related radioactivity was shown to be mainly cleared via the kidneys following dosing of [^{3}H]PEG or [^{3}H]N8-GP. PEGs of all MW are predominantly excreted unchanged in the urine, though at various rates depending on their size. 40 kDa PEG has been shown to be slowly eliminated from the body, mainly via renal elimination and likely by passive filtration (Nakaoka et al., 1997; Woodburn et al., 2013; Yamaoka et al., 1994). For [^{3}H]N8-GP, though not confirmed in these studies, it is unlikely that radioactivity found in rat urine would represent intact N8-GP as both the conjugate and rFVIII have MW much higher than the reported cut-off for kidney elimination (~70 kDa; (Caliceti and Veronese, 2003).

As seen by others (Cai et al., 2012; Nesbitt et al., 2009; Webster et al., 2009), hepatobiliary elimination appeared to be minor for [^{3}H]PEG, with only a small fraction of radioactivity recovered in feces. Furthermore, 40 kDa PEG is not believed to be extensively metabolized in the liver (Webster et al., 2007).

Cumulative excreta data of 1 and 200 mg/kg [^{3}H]PEG indicated similar fecal excretion of radioactivity, but dose-dependent urinary excretion (Fig. 3). Though the terminal excretion rates between 2 and 12 weeks post-dose were different between the two high doses and the lower doses, the main distinction appeared to be in the much larger fraction of radioactivity excreted into urine during the first 2 weeks for the lower doses.

Plasma data also showed dose-dependent kinetics of [^{3}H]PEG-related radioactivity after i.v. dosing of [^{3}H]PEG. This was evident in a slower terminal elimination rate following the 100 and 200 mg/kg doses compared to the dose levels of 12 mg/kg and below. There was a ~2-fold longer terminal $t_{½}$ for the top doses (42–59 days) versus 1 and 12 mg/kg (24–26 days) and also a larger fraction of dose remaining to be excreted from plasma 12 weeks post-dose. The latter observation was further confirmed by the larger fraction of radioactivity found in the animal carcasses for the top doses compared to the lower dose levels at week 12 (20% vs. 5%). At 0.6 mg/kg [^{3}H]PEG, an even faster elimination of radioactivity was indicated compared to the 1 and 12 mg/kg doses. Overall, the terminal $t_{½}$ for [^{3}H]PEG was found to be in line with results published in the literature e.g., for Cimzia where a $t_{½}$ ~23 days was found for the 40 kDa PEG moiety in certolizumab pegol following a s.c. dose of 400 mg/kg (Nesbitt et al., 2009).

Using modeling, one possible explanation compatible with the observed nonlinearity in [^{3}H]PEG-related radioactivity plasma data could be a wider peripheral distribution of the dosed radioactivity for the higher dose levels, with approximately 2-fold larger estimates of V_p compared to at the lower dose levels.

The low levels of radioactivity that remained to be excreted 12 weeks post-dose for both compounds were detected in several tissues/organs and were, thus, not confined to one specific location. The liver, lymph, and spleen contained much higher levels of radioactivity following administration of [^{3}H]N8-GP versus [^{3}H]PEG. The higher concentrations detected in the liver (including bile ducts) could be due to uptake via LRP.

The relatively high levels of radioactivity observed in the tissues related to the lymphatic system (lymph, mandibular lymph node, and spleen) following administration of [^{3}H]PEG, and especially [^{3}H]N8-GP (Fig. 2), indicate a role for lymphatic uptake in the disposition of PEG and especially of N8-GP. Interestingly, several publications describe similar observations for other PEGylated molecules, suggesting that PEGylation of proteins appears to promote extravasation and subsequent reabsorption of the conjugate into the lymphatics via the interstitial space after i.v. dosing. A relationship between higher PEG MW and increased lymphatic redistribution has also been described (Kaminskas et al., 2013; Lamka et al., 1995; Zou et al., 2013).

In conclusion, after single i.v. administration to the rat, [^{3}H]PEG-related radioactivity was shown to be widely distributed after both i.v. dosing of [^{3}H]N8-GP and [^{3}H]PEG, mainly in highly vascularized tissues, with the lowest levels found in the CNS. Though a slow elimination of radioactivity was observed over the 12-week study period, approximately half of the radioactive dose of either compound was removed from the body 1 week post-dose.

The radioactivity was eliminated mainly via the kidneys into urine but also via the liver into feces, with a larger fraction found in the feces for [^{3}H]N8-GP compared to [^{3}H]PEG. Elimination of the radioactivity related to the 40 kDa PEG-moiety was shown to be dose-dependent, with faster elimination at lower dose levels. The clinical dose of N8-GP provides a substantially lower PEG exposure (50–75 U/kg; PEG load of <0.002 mg/kg) when compared to the PEG doses investigated in this paper (0.03–200 mg/kg). This may imply an even faster clearance of the PEG-moiety after N8-GP administration of clinically relevant doses.

Authorship Contributions

Participated in research design: Bjørnsdottir, Kappers, Kornø, Kristensen, Bagger.

Conducted experiments: Selvig.

Contributed new reagents or analytic tools: None.

Performed data analysis: Bjørnsdottir, Sternebring.

Wrote or contributed to the writing of the manuscript: Bjørnsdottir, Sternebring, Kappers, Kristensen, Bagger.

Acknowledgments

The authors thank Marianne Kjalke, Novo Nordisk A/S, for the in vitro activity analysis, Covance (Harrogate, UK) for conducting all in vivo ADME studies described in this paper, and Thomas Krogh-Meibom, Novo Nordisk A/S, for the ELISA analysis.

References

MASAC Recommendation Concerning Prophylaxis. Document #179, 2007. Medical and Scientific Advisory Council. http://www.hemophilia.org/NHFWeb/MainPgs/MainNHF.aspx?menuid=57&contenid=1007.

Agerso, H., Stennicke, H.R., Pelzer, H., Olsen, E.N., Merricks, E.P., Defriess, N.A., Nichols, T.C., Ezban, M., 2012. Pharmacokinetics and pharmacodynamics of turoctocog alfa and N8-GP in haemophilia A dogs. Haemophilia 18, 941–947.

Bailon, P., Won, C.Y., 2009. PEG-modified biopharmaceuticals. Expert Opin. Drug Deliv. 6, 1–16.

Baumann, A., Tuerck, D., Prabhu, S., Dickmann, L., Sims, J., 2014. Pharmacokinetics, metabolism and distribution of PEGs and PEGylated proteins: quo vadis? Drug Discov. Today 19, 1623–1631.

Bjorkman, S., Berntorp, E., 2001. Pharmacokinetics of coagulation factors: clinical relevance for patients with haemophilia. Clin. Pharmacokinet. 40, 815–832.

Bjorkman, S., Folkesson, A., Jonsson, S., 2009. Pharmacokinetics and dose requirements of factor VIII over the age range 3–74 years: a population analysis based on 50 patients with long-term prophylactic treatment for haemophilia A. Eur. J. Clin. Pharmacol. 65, 989–998.

Bovenschen, N., Herz, J., Grimbergen, J.M., Lenting, P.J., Havekes, L.M., Mertens, K., van Vlijmen, B.J., 2003. Elevated plasma factor VIII in a mouse model of low-density lipoprotein receptor-related protein deficiency. Blood 101, 3933–3939.

Cai, Y., Zhang, Z., Fan, K., Zhang, J., Shen, W., Li, M., Si, D., Luo, H., Zeng, Y., Fu, P., Liu, C., 2012. Pharmacokinetics, tissue distribution, excretion, and antiviral activity of pegylated recombinant human consensus interferon-alpha variant in monkeys, rats and guinea pigs. Regul. Pept. 173, 74–81.

Caliceti, P., Veronese, F.M., 2003. Pharmacokinetic and biodistribution properties of poly(ethylene glycol)-protein conjugates. Adv. Drug Deliv. Rev. 55, 1261–1277.

Christiansen, M.L., Balling, K.W., Persson, E., Hilden, I., Bagger-Sorensen, A., Sorensen, B.B., Viuff, D., Segel, S., Klausen, N.K., Ezban, M., Lethagen, S., Steenstrup, T.D., Kjalke, M., 2010. Functional characteristics of N8, a new recombinant FVIII. Haemophilia 16, 878–887.

Coppola, A., Di, C.M., De, S.C., 2008. Primary prophylaxis in children with haemophilia. Blood Transfus. 6 (Supplement 2), S4–11.

Coppola, A., Franchini, M., 2013. Target of prophylaxis in severe haemophilia: more than factor levels. Blood Transfus. 11, 327–329.

DeFrees, S., Wang, Z.G., Xing, R., Scott, A.E., Wang, J., Zopf, D., Gouty, D.L., Sjoberg, E.R., Panneerselvam, K., Brinkman-Van der Linden, E.C., Bayer, R.J., Tarp, M.A., Clausen, H., 2006. GlycoPEGylation of recombinant therapeutic proteins produced in Escherichia coli. Glycobiology 16, 833–843.

Elliott, V.L., Edge, G.T., Phelan, M.M., Lian, L.Y., Webster, R., Finn, R.F., Park, B.K., Kitteringham, N.R., 2012. Evidence for metabolic cleavage of a PEGylated protein in vivo using multiple analytical methodologies. Mol. Pharm. 9, 1291–1301.

Harris, J.M., Chess, R.B., 2003. Effect of pegylation on pharmaceuticals. Nat. Rev. Drug Discov. 2, 214–221.

Hay, C.R., 2007. Prophylaxis in adults with haemophilia. Haemophilia 13 (Supplement 2), 10–15.

Ivens, I.A., Baumann, A., McDonald, T.A., Humphries, T.J., Michaels, L.A., Mathew, P., 2013. PEGylated therapeutic proteins for haemophilia treatment: a review for haemophilia caregivers. Haemophilia 19, 11–20.

Kaminskas, L.M., Ascher, D.B., McLeod, V.M., Herold, M.J., Le, C.P., Sloan, E.K., Porter, C.J., 2013. PEGylation of interferon alpha2 improves lymphatic exposure after subcutaneous and intravenous administration and improves antitumour efficacy against lymphatic breast cancer metastases. J. Control. Release 168, 200–208.

Lamka, J., Schiavon, O., Laznicek, M., Caliceti, P., Veronese, F.M., 1995. Distribution of catalase, ribonuclease and superoxide dismutase modified by monomethoxy (polyethylene glycol) into rat central lymph and lymphatic nodes. Physiol. Res. 44, 307–313.

Malmstrom, J., 2012. Characterization of 40 kDa poly(ethylene glycol) polymers by proton transfer reaction QTOF mass spectrometry and 1H-NMR spectroscopy. Anal. Bioanal. Chem. 403, 1167–1177.

Mei, B., Pan, C., Jiang, H., Tjandra, H., Strauss, J., Chen, Y., Liu, T., Zhang, X., Severs, J., Newgren, J., Chen, J., Gu, J.M., Subramanyam, B., Fournel, M.A., Pierce, G.F., Murphy, J.E., 2010. Rational design of a fully active, long-acting PEGylated factor VIII for hemophilia A treatment. Blood 116, 270–279.

Nakaoka, R., Tabata, Y., Yamaoka, T., Ikada, Y., 1997. Prolongation of the serum half-life period of superoxide dismutase by poly(ethylene glycol) modification. J. Control. Release 46, 253–261.

Nesbitt, A.M., Stephens, S., Chartash, E.K., 2009. Certolizumab Pegol: A PEgylated Anti-Tumour Necrosis Factor Alpha Biological Agent. PEGylated Protein Drugs: Basic Science and Clinical Applications.

Nilsson, I.M., Berntorp, E., Lofqvist, T., Pettersson, H., 1992. Twenty-five years' experience of prophylactic treatment in severe haemophilia A and B. J. Intern. Med. 232, 25–32.

Saenko, E.L., Yakhyaev, A.V., Mikhailenko, I., Strickland, D.K., Sarafanov, A.G., 1999. Role of the low density lipoprotein-related protein receptor in mediation of factor VIII catabolism. J. Biol. Chem. 274, 37685–37692.

Srivastava, A., Brewer, A.K., Mauser-Bunschoten, E.P., Key, N.S., Kitchen, S., Llinas, A., Ludlam, C.A., Mahlangu, J.N., Mulder, K., Poon, M.C., Street, A., 2013. Guidelines for the management of hemophilia. Haemophilia 19, e1–47.

Stennicke, H.R., Kjalke, M., Karpf, D.M., Balling, K.W., Johansen, P.B., Elm, T., Ovlisen, K., Moller, F., Holmberg, H.L., Gudme, C.N., Persson, E., Hilden, I., Pelzer, H., Rahbek-Nielsen, H., Jespersgaard, C., Bogsnes, A., Pedersen, A.A., Kristensen, A.K., Peschke, B., Kappers, W., Rode, F., Thim, L., Tranholm, M., Ezban, M., Olsen, E.H., Bjorn, S.E., 2013. A novel B-domain O-glycoPEGylated FVIII (N8-GP) demonstrates full efficacy and prolonged effect in hemophilic mice models. Blood 121, 2108–2116.

Strickland, D.K., Au, D.T., Cunfer, P., Muratoglu, S.C., 2014. Low-density lipoprotein receptor-related protein-1: role in the regulation of vascular integrity. Arterioscler. Thromb. Vasc. Biol. 34, 487–498.

Tiede, A., Brand, B., Fischer, R., Kavakli, K., Lentz, S.R., Matsushita, T., Rea, C., Knobe, K., Viuff, D., 2013. Enhancing the pharmacokinetic properties of recombinant factor VIII: first-in-human trial of glycoPEGylated recombinant factor VIII in patients with hemophilia A. J. Thromb. Haemost. 11, 670–678.

Turecek, P.L., Bossard, M.J., Graninger, M., Gritsch, H., Hollriegl, W., Kaliwoda, M., Matthiessen, P., Mitterer, A., Muchitsch, E.M., Purtscher, M., Rottensteiner, H., Schiviz, A., Schrenk, G., Siekmann, J., Varadi, K., Riley, T., Ehrlich, H.J., Schwarz, H.P., Scheiflinger, F., 2012. BAX 855, a PEGylated rFVIII product with prolonged half-life. Development, functional and structural characterisation. Hamostaseologie 32 (Supplement 1), S29–S38.

Webster, R., Didier, E., Harris, P., Siegel, N., Stadler, J., Tilbury, L., Smith, D., 2007. PEGylated proteins: evaluation of their safety in the absence of definitive metabolism studies. Drug Metab. Dispos. 35, 9–16.

Webster, R., Elliott, V., Park, B.K., Walker, D., Hankin, M., Taupin, P., 2009. PEG and PEG Conjugates Toxicity: Towards an Understanding of the Toxicity of PEG and its Relevance to PEGylated Biologicals. PEGylated Protein Drugs: Basic Science and Clinical Applications.

Woodburn, K.W., Fong, K.L., Wilson, S.D., Sloneker, S., Strzemienski, P., Solon, E., Moriya, Y., Tagawa, Y., 2013. Peginesatide clearance, distribution, metabolism, and excretion in monkeys following intravenous administration. Drug Metab. Dispos. 41, 774–784.

Yamaoka, T., Tabata, Y., Ikada, Y., 1994. Distribution and tissue uptake of poly(ethylene glycol) with different molecular weights after intravenous administration to mice. J. Pharm. Sci. 83, 601–606.

Zou, Y., Bateman, T.J., Adreani, C., Shen, X., Cunningham, P.K., Wang, B., Trinh, T., Christine, A., Hong, X., Nunes, C.N., Johnson, C.V., Zhang, A.S., Staskiewicz, S.J., Braun, M., Kumar, S., Reddy, V.B., 2013. Lymphatic absorption, metabolism, and excretion of a therapeutic peptide in dogs and rats. Drug Metab. Dispos. 41, 2206–2214.